On plasma coupling and turbulence effects in low velocity stopping

Yu K Kurilenkov[1], G Maynard[2], M D Barriga-Carrasco[2] and A A Valuev[1]

[1] Unified Institute for High Temperatures of Russian Academy of Sciences, 13/19 Izhorskaya Str., 125412 Moscow, Russia
[2] Laboratoire de Physique des Gaz et des Plasmas, UMR-8578, Bât. 210, Université Paris XI, F-91405 Orsay, France

E-mail: ykur@online.ru

Abstract
The problem of stopping power (SP) for projectile ions is analysed in terms of the dielectric function and effective collision frequency for moderately dense and strongly coupled plasmas (SCP). We consider several issues regarding the calculation of stopping power for correlated ensembles of particles and oscillators. In particular, effects of group (few particle) modes, transition from positive to negative dispersion and excitation of collective modes up to suprathermal level at plasma targets are addressed. Linear SP of dense suprathermal (nonlinear) plasma targets at different levels of target plasma turbulence is estimated. The force of suprathermal plasma oscillations on the projectile ions is mostly in the nature of increased frictional drag. The results obtained show the possibility of increasing low velocity stopping (up to 'turbulent' values) in comparison with losses in equilibrium dense plasma targets. Experimental conditions to create specific turbulent targets as well as some connection between stopping phenomena and SCP transport properties are discussed briefly.

PACS numbers: 34.50.Bw, 52.20.Hv, 52.40.Mj

1. Introductory remarks

The dielectric description is one of the efficient and frequently used ways to describe the optical properties of the matter [1] as well as to investigate the specifics of energy losses of any charged particles passing through the matter [2–4]. In fact, stopping power (SP), or average energy loss per unit path length, is a consequence of the retarding force acting on projectile due to a self-induced electric field. The dielectric formalism (see for instance [2–6] and references therein) provides a way to calculate the induced electric field at the instantaneous position

of moving ion (with charge Z and velocity V_0). On the basis of linear response theory the expression for the stopping power of a particular medium is found to be

$$\text{SP} \approx \frac{2Z^2}{\pi V_0^2} \int_0^\infty \frac{\mathrm{d}k}{k} \int_0^{kV_0} \mathrm{d}\omega \, \omega \, \text{Im}\left(\frac{-1}{\varepsilon(k,\omega)}\right), \tag{1}$$

where $\varepsilon(k,\omega)$ is the wave vector (k) and frequency (ω) dependent dielectric function of the medium. Moderately dense and strongly coupled plasmas (SCP) represent the fundamental interest for modern high energy density physics, and the corresponding SP under special or extreme conditions is a subject of detailed study [6–8]. Generally, the coupled plasma targets [6] under consideration are characterized by the coupling parameter $\Gamma = e^2\beta/a$, where $\beta = 1/kT$, and $a = (3/4\pi n_i)^{1/3}$, and the degeneracy parameter $\vartheta = 1/\beta T_{\text{F}}$, as well as by the level of plasma oscillations (plasma turbulence) $\xi = \langle E^2 \rangle / 8\pi nT$ (where E is the strength of the plasma oscillation fields) [9]. At the thermal level of oscillations for dilute or rather dense plasmas we have $\xi_{\text{therm}} \ll 1$, but ξ increases with Γ. Meanwhile, some plasma instabilities may provoke the values $\xi \gg \xi_{\text{therm}}$ even for collision-dominated plasmas [9–13].

We consider coupled plasma target conditions where the free plasma electrons give the main contribution to SP. In general, the key quantities needed for proper calculations of the energy loss function, $\text{Im}(-1/\varepsilon(k,\omega))$, are the dielectric function of plasma and the dynamic collision frequency $\nu(k,\omega)$. The latter is the subject of rather standard approximations, starting from $\nu \cong 0$, $\nu \cong \text{const}$, $\nu \cong \nu(\omega)$, etc. More sophisticated calculations of $\nu(k,\omega)$ in a wide range of k and ω require special efforts [13, 14]. Recognizing that the dynamic collision frequency may also depend on the level of plasma oscillations, we conclude that the parameters Γ, ϑ and ξ do influence the energy loss functions (ELF) in the plane (k,ω), providing the spectrum of the corresponding conditions for SP at different projectile velocities. In other words, the density and correlations effects, as well as any plasma collective mode excitations in the plane (k,ω), will effect the ELF and related values of integrals of the SP expression. Regarding the descriptive character of ELF, we note that a particular value of SP in equation (1) at a fixed projectile velocity V_0 is proportional to the volume restricted by $\text{Im}(-1/\varepsilon(k,\omega))$ itself, and some vertical plane (which is perpendicular to the plane (k,ω)) turned with the angle $\sim V_0$. Thus, for example, different dense plasma target conditions such as weak or strong plasma coupling, thermal or suprathermal level of plasma oscillations, and positive or negative plasma dispersion will manifest themselves at this ELF 'map' and even a visual view of ELF could be useful to predict specifics or estimate the value of particular SP.

As indicated above knowledge or choice of $\varepsilon(k,\omega)$ and $\nu(\omega)$ for a dense plasma target with particular properties provides the value of SP. The main purpose of the present work is to estimate for a correlated plasma target the possible role of suprathermal plasma oscillations (or plasma 'turbulence') in the stopping of ions ($Z = 1$). Examples of different energy loss functions and SP values estimated are presented in figures 1–8 and discussed below in an attempt to illustrate some manifestations of correlations as well as plasma 'turbulence' effects in stopping for a coupled, non-degenerate plasma target.

2. Energy loss functions

We start the analysis from the well-known ELF in random phase approximation (RPA) [15] (figure 1). The single-particle excitations and undamped ($\nu = 0$) collective excitations are represented by RPA (the latter ones are beyond the scope in figure 1 since they are expressed by δ-functions on the dispersion curve $\omega(k)$ from $\omega = \omega_{\text{pl}}$ at $k \to 0$). This 'ideal' ELF is useful as a reference for further comparisons with an RPA including collisions [16, 17]. Looking forward, the model ELF [17] reproduces some contours of the RPA ELF, as shown in
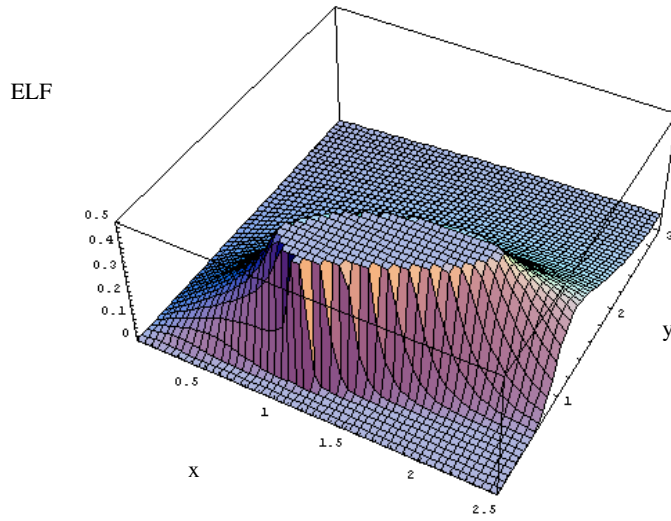
Figure 1. Energy loss function (ELF) as a function of ω and k in RPA [15] ($x = \omega/\omega_{\text{pl}}$, $y = kr_0$).
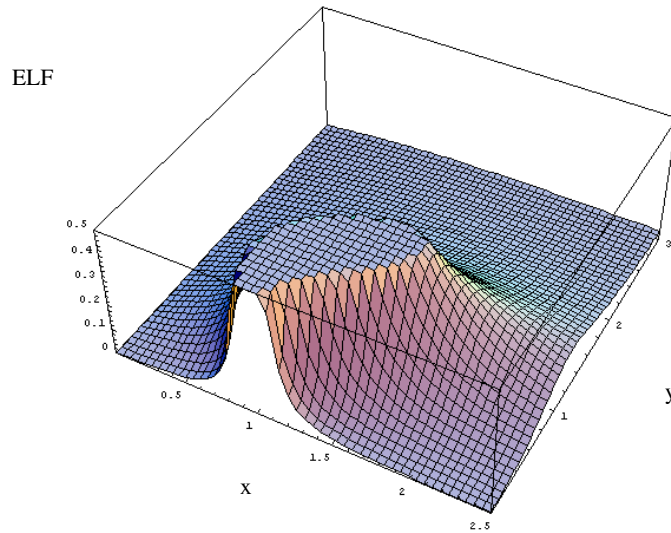

Figure 2. Non-equilibrium ELF at $\Gamma = 0.3$, $\vartheta = 5$ for $\xi > \xi_{\text{therm}}$ ($\xi = 0.1$) with $\varepsilon(k, \omega)$ from BK [17] ($\xi_{\text{therm}} \approx 0.02$) ($x = \omega/\omega_{\text{pl}}$, $y = kr_0$) (see the related value of SP in figure 4, curve 2).

figures 2 and 3 for moderate coupling ($\Gamma = 0.3$). It takes place due to the introduction of excitations of plasma oscillations up to suprathermal levels $\xi \gg \xi_{\text{therm}}$ ($\xi = 0.1$ and $\xi = 1$, respectively). Collisions have also been introduced. They decrease the amplitude and increase the width of plasma resonances that will influence SP values correspondingly (figures 4, 6 and 8 discussed below).

A version of the RPA with collisions ($\nu \neq 0$) was suggested by Mermin [16], where the final lifetime for plasmons has been introduced by a consistent way. In general, the Mermin function has the property of a useful 'shell' for the ELF if the wave damping decrement is chosen reasonably, including the dependence on k and ω. As an example, figure 5 shows
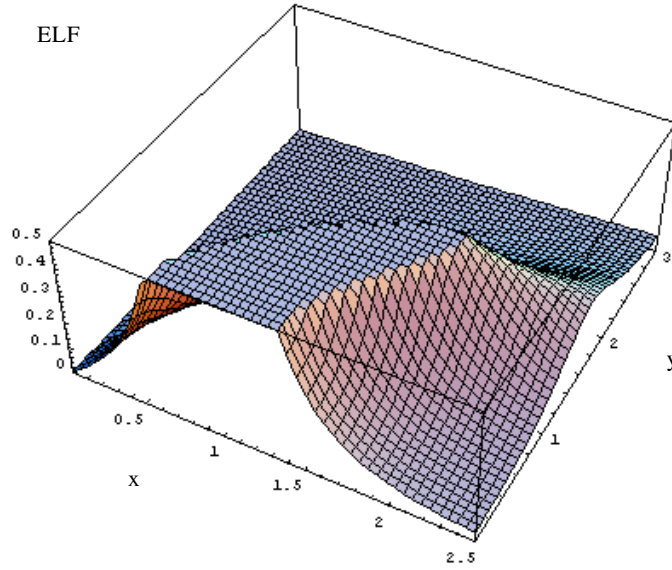
ELF

Figure 3. Non-equilibrium ELF at $\Gamma = 0.3$, $\vartheta = 5$ for $\xi > \xi_{\text{therm}}$ (BK, $\xi = 1$; $\xi_{\text{therm}} \approx 0.02$; $x = \omega/\omega_{\text{pl}}$, $y = kr_0$) (see the corresponding SP in figure 4, curve 3).
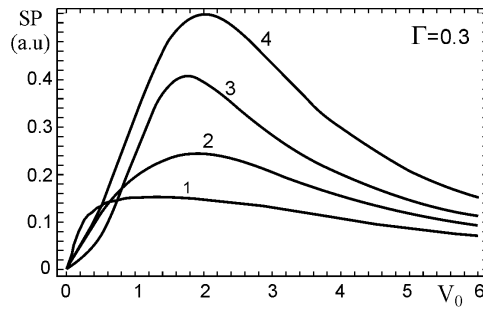

Figure 4. Stopping power (au) at $\Gamma = 0.3$, $\vartheta = 5$. Curve 1: thermal target SP, $\xi = 0.02$; curve 2: supra-thermal $\xi = 0.1$; curve 3: $\xi = 1$; curve 4: RPA (here and below V_0 in units of v_{th}^e).

the Mermin [16] ELF, where the plasma wave damping decrement was taken from a quasi hydrodynamical model (see below, BK [17]). The dielectric function based on the quasi hydrodynamical model has been obtained earlier [17] (also, specifics of plasmon dispersion and damping of plasma oscillations at $\Gamma \sim 1$ have been discussed in detail [12, 17]). In fact, the Mermin ELF presented in figure 5 for $\Gamma = 1$ is almost the same as that based on the simple BK model dielectric function (equation (7) of [17]), where the specifics of collective modes in the SCP as well as modified binary collisions were taken into account. Thus, as in figures 2 and 3, we will further use the BK model to simplify the ELF and SP calculations under rather transparent stopping physics.

In the BK model (see also review [12] for details) the total decrement of plasma oscillations has been presented as $\delta_{\text{BK}} \approx \delta_{\text{Coll}} + \delta_{\text{NR}}$, where $\delta_{\text{Coll}} \sim \tau_{ee}\nu_{\text{eff}}^2$ is the collision damping due to modified binary collisions as well as non-pair scattering by collective oscillations ($\nu_{\text{eff}} \approx \nu_{ei}^* + \xi_{\text{therm}}\omega_{\text{pl}}$, τ_{ee} is the time of e–e correlations, $\nu_{ei}^* \sim \Gamma^{3/2}\,\omega_{\text{pl}}\,\ln\,(1 + 9/4\,\Gamma^3)$, $\delta_{\text{NR}}/\omega_{\text{pl}} \sim (ka)^2/\xi_{\text{therm}}^{1/2}$ is the non-resonant wave damping [17]). Despite the increase
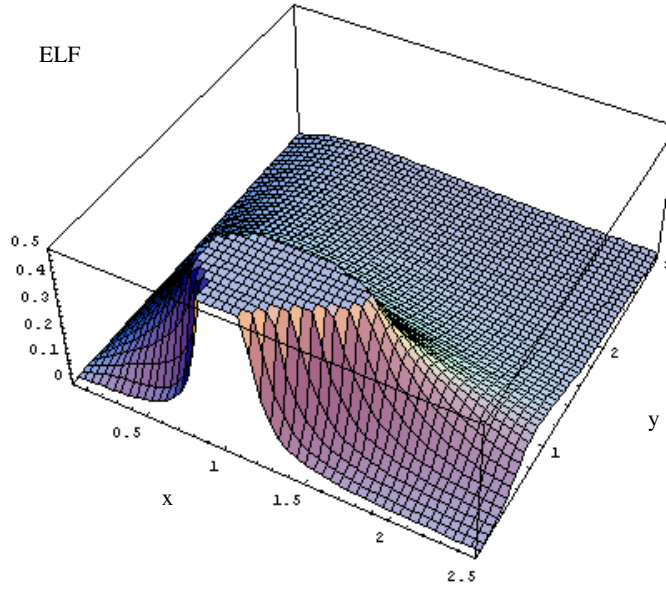
Figure 5. Mermin [16] ELF $\mathrm{Im}(-1/\varepsilon(k,\omega))$ with BK damping decrement [17] at $\Gamma = 1$, $\vartheta = 5$ (ELF is very close to ELFs from BK [17], which is not shown; $x = \omega/\omega_{pl}$, $y = kr_0$) (see SP in figure 6, curve 2).
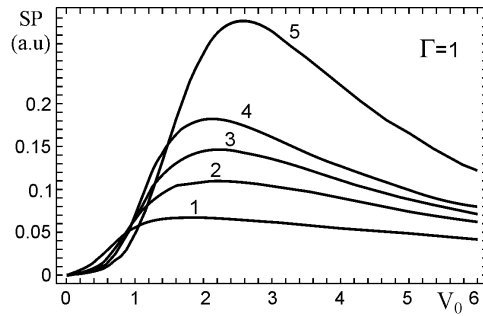

Figure 6. Stopping power (au) at $\Gamma = 1$, $\vartheta = 5$. Curve 1: well-defined modes only, $ka \leqslant 1$, $\xi_{\mathrm{well\text{-}def}} \approx 0.024$; curve 2: thermal SP, $\xi_{\mathrm{therm}} \approx 0.12$; curve 3: $\xi = 0.3$; curve 4: $\xi = 1$; curve 5: RPA.

in δ_{Coll} with Γ, its values are lower than ω_{pl} even at $\Gamma \sim 1$. Besides, ion–ion correlations act to decrease the collisional damping. Non-resonant wave damping appears at $\Gamma \geqslant 0.3$ [12, 17]. Its nature is reminiscent of viscous damping of sound waves in condensed media, where all the oscillating particles contribute to wave damping. The reason for this non-resonant damping is the diffusion of electron momentum. In fact, as the coupling increases the electron–electron collision frequency increases and electrons have to begin exchanging momentum during the period of plasma oscillations, $\tau_{ee} \leqslant T = 2\pi/\omega_{pl}$. As a result, the energy of the electron directed motion obtained in the field of the wave will transfer into heat due to collisions. This type of dissipation has been called non-resonant, since all oscillating electrons participate in this process (in contrast to Landau resonant damping in a dilute plasma). These different mechanisms of damping (Landau, $\Gamma \leqslant 0.3$, and non-resonant, $\Gamma \geqslant 0.3$) are almost non-overlapping, and their self-influence should be slightly noticeable just at transition values
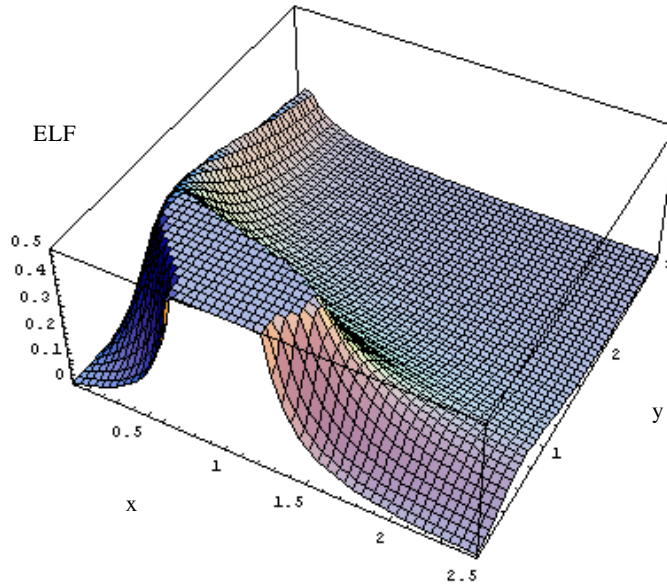
Figure 7. ELF at $\Gamma = 2$, $\vartheta = 5$ with $\partial\omega/\partial k \leqslant 0$ (BK, $\xi_{\text{therm}} \approx 0.33$; $x = \omega/\omega_{\text{pl}}$, $y = kr_0$) (see the corresponding SP in figure 8, curve 2).
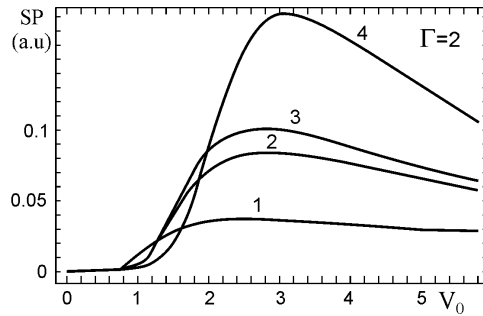

Figure 8. Stopping power (au) at $\Gamma = 2$, $\vartheta = 5$. Curve 1: well-defined modes only, $ka \leqslant 1$, $\xi_{\text{well-def}} \approx 0.024$; curve 2: thermal SP, $\xi_{\text{therm}} \approx 0.33$; curve 3: $\xi = 1$; curve 4: RPA.

of coupling ($\Gamma \approx 0.3$). Note that at $ka = $ constant, the value δ_{NR} decreases at higher Γ (since the value $\tau_{\text{ee}} \sim 1/\omega_{\text{pl}}\xi_{\text{therm}}^{1/2}$ decreases [17]). These specifics of the damping of plasma oscillation at collision-dominated plasmas have been recognized even in early MD simulations of two-component SCP [18], and less obviously so in the recently available MD data also [19].

Another related feature of dense plasma oscillations at $\Gamma \geqslant 0.3$ is the appearance of an area of *group modes*, $r_0 \leqslant k^{-1} \leqslant a$ [12, 17]. In fact, as Γ grows, the Debye screening radius $r_0 \approx v_{\text{Te}}/\omega_{\text{pl}}$ decreases and r_0 formally becomes less than the interparticle distance a. Thus, the parameter r_0 loses the meaning of a screening parameter, while the relation $v_{\text{Te}}/\omega_{\text{pl}}$ will keep the sense of a maximum possible space amplitude r_{osc} of plasma oscillations, $r_{\text{osc}}/r_0 \approx \xi^{1/2}$, even at strong coupling. Electron screening is established on a scale of the order of the mean interparticle distance a, and in such a nonideal plasma collective modes can exist in the domain $a \leqslant k^{-1}$. One might expect that fluctuations $k^{-1} \leqslant a$ have an individual character. However, results of MD simulations demonstrate that modes $r_0 \leqslant k^{-1} \leqslant a$ retain some characteristics of

plasma oscillation [18]. Although such oscillations are strongly damped, they are revealed as distinct maxima of the dynamic structure factor at frequencies $\omega \sim \omega_{pl}$. Such modes appear as a result of interaction with a few neighbouring particles. Namely, group modes will contain the main part of the energy of oscillations in a SCP, $\xi_{therm} \sim 0.1\Gamma^{3/2}$, while the energy of well-defined modes ($a \leqslant k^{-1}$) has to be saturated approximately at the level of $\xi_{well-def} \approx 0.024$ in spite of increasing Γ [10, 17].

The dispersion relation of plasma oscillations $\omega(k) = \omega_{pl}(1 + A(\Gamma)k^2r_0^2)$, where $A(\Gamma)$ exhibits a linear decrease with Γ, manifests a transition to negative dispersion at $\Gamma \approx 2$ [12]. This property of plasmon dispersion at strong coupling has been recognized earlier in the framework of the OCP model, as well as being observed in MD simulations (see [20] and references therein). The thermal ELF by BK as presented in figure 7 was extrapolated to $\Gamma = 2$ and clearly illustrates the *transition to negative dispersion*, $\partial\omega/\partial k \leqslant 0$ (the particular dispersion curves were presented and discussed earlier [17]). Negative dispersion may provide a relative increase of SP at low projectile velocities due to the 'tail' of ELF extending into the area of $\omega \leqslant \omega_{pl}$ and group modes (figure 7). Perhaps it would also be especially important for SP at rather high projectiles densities, when beam-plasma instabilities could be accompanied by a changing sign for the group velocity of excitations [7, 21].

Thus, with Γ increasing (like from figure 5 to figure 7) the *thermal* ELF has a tendency of evolution from rather well-pronounced group modes, $kr_0 \leqslant 1$ (figure 5), into the area of certain negative plasmon dispersion $\omega \leqslant \omega_{pl}$ at a group mode area, $kr_0 \sim 1$ (ELF perturbed to the left in the (k, ω) plane). Meanwhile, *suprathermal* ELF with excited plasma modes $\xi \gg \xi_{therm}$ have a tendency to approach RPA values (ELF perturbed to the right in the (k, ω) plane). The last one simply means that undamped plasma oscillations incorporated into the RPA derivation [15] are similar in some sense to manifestations of forced or induced oscillations. If any induced instability at the SCP target is strong enough, we may get ELF values almost like in the case of RPA, in spite of coupling effects. The corresponding consequences have also to be pronounced at SP values.

3. 'Turbulent' stopping

Earlier, analysis of SCP experimental and simulation data has shown [11, 22–26] that in spite of the collision-dominated character SCP may manifest the anomalous transport properties ($\nu_{eff} \rightarrow \omega_{pl}$) related to excitation of plasma turbulence, $\xi \gg \xi_{therm}$, while under equilibrium conditions we have $\nu_{eff} \sim \xi_{therm}\omega_{pl}$ [23]. The related possible anomalous effects are the subject of the present study for SCP transport and optical properties such as conductivity, reflectivity and plasma opacity [11, 12, 19, 22–26]. Meanwhile, the direct connection between the SP and collision frequency $\nu(\omega)$ at the low frequency limit, $SP \sim V_0\nu_s$, with $\nu_s = \nu(0)$, can be accomplished [25]. This result can also be derived by writing the low velocity stopping and collision frequency in terms of the force–force correlation function [27]. It means that the electron subsystem scattering by plasma ions is similar to the inverse problem—low velocity ion stopping by the electron subsystem even at strong coupling (like understanding Cherenkov radiation makes clearer the nature of Landau damping). Note that the nonlinear stopping expression given in [28] is recovered by calculating the dynamic collision frequency $\nu(\omega)$ in the three-term approximation (TTA) [13], where an ansatz according to Gould and DeWitt [29] has been used. Only the binary collision term remains at the low velocity limit at a combined model for nonlinear stopping [28]. Correspondingly, SP at the low velocity limit may be rewritten in terms of the static conductivity $\sigma_s = \omega_{pl}^2/4\pi\nu_s$ [25]

$$SP/V_0 \, \omega_{pl} = \omega_{pl}/4\pi \, \sigma_s. \tag{2}$$

It means that anomalously low transport like anomalous conductivity $\sigma_{\text{lim}} \approx \omega_{\text{pl}}/4\pi$ [22, 23] under some instabilities developed in the plasma target has to be accompanied by anomalously high stopping in the low velocity limit,

$$\text{SP}_{\text{lim}} \approx V_0 \, \omega_{\text{pl}}. \tag{3}$$

Thus, probably the different target conditions such as weak or strong coupling could be extended due to 'turbulent' plasma targets.

Let us try to estimate the linear response (losses) from the nonlinear turbulent SCP target (in the low velocity domain $V_0 \sim v_{\text{th}}$), when a suprathermal level of oscillation $\xi \gg \xi_{\text{therm}}$ is introduced into ELF as discussed above. In fact, the fluctuation-dissipation theorem [9] connects the equilibrium properties of a plasma with irreversible processes (losses),

$$2\pi\omega\beta \, k^{-2} \, S_{zz} \, (k, \omega) = \text{Im}(-1/\varepsilon(k, \omega), \tag{4}$$

where $S_{zz}(k, \omega)$ is the dynamic structure factor. Recall that $\xi(k, \omega) \sim S_{zz}(k, \omega)$, and integration of $S_{zz}(k, \omega)$ over k and ω provides the value of ξ_{therm}, i.e. the losses and oscillations are in correlation in thermal plasmas. The properties of a 'turbulent' target like $\xi \gg \xi_{\text{therm}}$ might be included into a linear $\varepsilon(k, \omega)$ if we consider the non-equilibrium target under rather 'stable' conditions (when any externally provoked instability is not developing further [9]). Thus, we can estimate *linear losses* from the externally formed *nonlinear target* (with suprathermal level of oscillations) [21].

Figures 2 and 3 illustrate the evolution of ELF (at $\Gamma = 0.3$) at increased suprathermal values $\xi = 0.1$ and $\xi = 1$. The corresponding SP values are shown in figure 4 by curves 2 and 3. Thus, the area between thermal SP (curve 1) and RPA (curve 4) could be 'fulfilled' by increasing the level of target 'turbulence' $\xi \gg \xi_{\text{therm}}$. The thermal SP for $\Gamma = 1$ (figure 6) and some extrapolation for $\Gamma = 2$ also (figure 8) are represented by curves 2, while the SP due to well-defined modes are shown by curves 1 in these figures. Hence, the difference between curves 1 and 2 represents the particular role of group modes at SP values. We see that their role in stopping may increase with Γ.

Thus, group modes $r_0 \leqslant k^{-1} \leqslant a$ could be essential both for thermal and 'turbulent' stopping at strong coupling (figures 6 and 8). Meanwhile, variation of the level of target 'turbulence' can influence SP, and it will be especially pronounced at moderate coupling like in figure 4. In comparison to the reference RPA stopping, two effects have to be noted. First, collisions in SCP decrease the amplitude and increase the widths of plasma resonances, which provokes a decrease of SP in general with growing Γ. Second, induced suprathermal values of $\xi \gg \xi_{\text{therm}}$ may partially compensate these effects and increase SP up to anomalous values (figures 4, 6 and 8) [25]. However, the difference between 'turbulent' SP (at $\xi \approx 1$) and RPA stopping increases with Γ because of a growing role of collisional damping in the target plasma. Calculations also show that at $\xi > 1$ the value of SP saturates at $\xi \approx 1$ (not shown in figures 4, 6 and 8), since the space amplitude $r_{\text{osc}} \sim \xi^{1/2}r_0$ does not exceed the value of $v_{\text{Te}}/\omega_{\text{pl}} \approx r_0$ [17, 23].

We remark that the upper limit of k_{max} was introduced in SP, equation (1), to account for physical effects at small distances [6] and not just to avoid divergences (the interpolation expression (5) discussed in [30] has been used here). However, the linear response description with cut-off k_{max} fails at $Z\Gamma^{3/2} \geqslant 1$, and linearity of SP at the low velocity limit is obviously being perturbed with growing Γ (figures 4 and 6). The introduction of k_{max} gives a simple way to extend linear response into the semilinear regime, but it works just close to the linear regime and has physical deficiencies also. For example, the interesting area of the negative dispersion of ELF at $\Gamma = 2$ will be almost ignored under this cutting. Nevertheless, our general conclusions about the role of group modes or suprathermal oscillations for SP values at $V_0 \geqslant$ 2–3v_{th} will be conserved and for strong coupling. On the other hand, for moderate coupling

($\Gamma = 0.3$) the excited area of ELF (figures 2 and 3) is far from k_{max} and linear response is sufficient to describe 'turbulent' stopping. Nevertheless, the k_{max} cutting procedure disturbs the values of SP at $V_0 \to 0$ and further steps towards the nonlinear regime have to be carried out beyond linear response (see discussions in [6, 8, 30]), as well as in parallel to rely on molecular dynamics simulations of SP for regimes $\xi \gg \xi_{therm}$ (see also [31] and references therein).

More generally, a strongly coupled non-equilibrium (turbulent) plasma represents an additional type of target for stopping which probably supplements the available list of target conditions (see table 1 of [6]). For a real experimental scheme the SCP instability that could be induced by external means (like current-carrying plasma (cf [24]), specially chosen laser–target or extra beam–target interactions, plasma pinches) has to be combined with the passing of projectile particles to realize 'turbulent' stopping. Moderately coupled plasmas (like in figure 4) with the external source of 'pumping' of oscillations up to suprathermal levels look rather suitable to check the role of turbulent stopping in experiment. Note that rather often experiments on the generation of dense or nonideal plasmas are accompanied by induced excitation of suprathermal waves $\xi \gg \xi_{therm}$ [22, 24, 26]. Thus, related data on transport, stopping and energy loss spectra for these experiments need further detailed analysis (particular examples are rather recent data for dense pinched plasmas [32] and isochoric heating of foils by protons [33]). On the other hand, further molecular dynamics calculations [19] which had recognized even at the early stage of dense plasma MD simulation the possibility of appearance of anomalous values of collision frequency ($\nu_{eff} \sim \omega_{pl}$ [11, 22]) could be essential to improve and estimate 'turbulent' SP values also.

Acknowledgments

References

[1] Landau L D and Lifshits E M 1992 *Electrodynamics of Continuous Media* (Moscow: Nauka)
[2] Fermi E 1924 *Z. Phys.* **29** 315
    Fermi E 1939 *Phys. Rev.* **56** 1242
    Fermi E 1940 *Phys. Rev.* **57** 485
[3] Rukhadze A A and Silin V P 1961 *Physics of Plasma and Plasma-Like Media* (Moscow: Atomizdat)
[4] Echinique P M, Ritchie R H and Brandt W 1979 *Phys. Rev.* B **20** 2567
[5] Abril I, Garcia-Molina R, Denton C D, Perez-Perez F and Arista N R 1998 *Phys. Rev. A* **58** 357
[6] Zwicknagel G, Toepffer Ch and Reinhard P-G 1999 *Phys. Rep.* **309** 117
[7] Gericke D O and Schlanges M 1999 *Phys. Rev.* E **60** 904
[8] Maynard G, Zwicknagel G, Deutsch C and Katsonis K 2001 *Phys. Rev. A* **63** 052903
[9] Alexandrov A F, Bogdankevich L S and Rukhadze A A 1988 *Plasma Electrodynamics* (Moscow: Visshaya Shkola)
[10] Valuev A A and Norman G E 1998 *Dokladi RAN* **362** 752
[11] Valuev A A and Norman G E 1979 *J. Plasma Phys.* **21** 531
[12] Kurilenkov Yu K and Berkovsky M A 1995 *Transport and Optical Properties of Nonideal Plasmas* ed G A Kobzev, I T Iakubov and M M Popovich (New York: Plenum) p 215
[13] Berkovsky M A and Kurilenkov Yu K 1993 *Physica* A **197** 676
[14] Millat Th, Selchow A, Wierling A, Reinholtz H, Redmer R and Röpke G 2003 *J. Phys. A: Math. Gen.* **36** 6259
[15] Pines D and Bohm D 1952 *Phys. Rev.* **85** 338
    Pines D 1964 *Elementary Excitations in Solids* (New York: Benjamin)
[16] Mermin N D 1970 *Phys. Rev.* B **1** 2362

[17] Berkovsky M A and Kurilenkov Yu K 1990 *J. Quant. Spectr. Rad. Trans.* **43** 25
     Berkovsky M A and Kurilenkov Yu K 1987 *Preprint* IVTAN I-223
[18] Hansen J P, McDonald I R and Pollock E L 1975 *Phys. Rev.* A **11** 1025
     Hansen J P and Sjogren L 1982 *Phys. Fluids* **25** 617
[19] Morozov I, Norman G E, Valuev A A and Valuev I A 2003 *J. Phys. A: Math. Gen.* **36** 8723
[20] Kalman G and Golden K I 1990 *Phys. Rev.* A **41** 5516
[21] Rukhadze A and Alexandrov A F 2002 *Lectures on Plasmas Electrodynamics – Nonequilibrium Media* (Moscow: Department of Physics of Moscow State University)
[22] Asinovskii E I and Valuev A A 1980 *High Temp.* **18** 1318
[23] Valuev A A and Kurilenkov Yu K 1984 *Beitr. Plasmaphys.* **4** 161
[24] Batenin V M, Berkovsky M A, Kurilenkov Yu K and Valuev A A 1987 *High Temp.* **25** 299
[25] Maynard G, Kurilenkov K and Dufty J 1998 *Strongly Coupled Coulomb Systems* ed G J Kalman, K Blagoev and M Rommel (New York and London: Plenum) p 547
[26] Kurilenkov Yu K and Berkovsky M A 1987 *Lett. JTPh* **13** 90
     Berkovsky M A, Kurilenkov Yu K and Milchberg H M 1992 *Phys. Fluids* B **4** 2423
     Kurilenkov K *et al* 1995 *J. Phys. B: At. Mol. Opt. Phys.* **28** 2021
[27] Dufty J and Berkovsky M A 1995 *Nucl. Instrum Meth. Phys. Res.* A **B96** 626
[28] Maynard G, Katsonis K, Zwicknagel G, Mabong S, Chabot M, Gardes D and Kurilenkov Yu K 1998 *Nucl. Instrum. Meth. Phys. Res.* A **415** 687
[29] Gold H A and DeWitt Y E 1967 *Phys. Rev.* **155** 68
[30] Zwicknagel G 2002 *Nucl. Instrum. Meth. Phys. Res.* B **197** 22
[31] Kalman G J and Rosenberg M 2003 *J. Phys. A: Math. Gen.* **36** 5963
[32] Ogawa M *et al* 2003 *Proc. 30th Euro. Conf. on Plasma Phys. Contr. Fusion (St. Petersburg)*
[33] Patel P K, Mackinnon A J, Key M H, Cowan T E, Foord M E, Allen M, Price D F, Ruhl H, Springer P T and Stephens R 2003 *Phys. Rev. Lett.* **91** 125004